Scale Invariance and Universality in a Cold Gas of Indirect Excitons

S. V. Andreev,[1,*] A. A. Varlamov,[2] and A. V. Kavokin[3,4]
[1]Laboratoire Charles Coulomb, Unité Mixte de Recherche 5221 CNRS/UM2, Université Montpellier 2, Place Eugne Bataillon, 34095 Montpellier Cedex, France
[2]CNR-SPIN, Tor Vergata, Viale del Politecnico 1, I-00133 Rome, Italy
[3]Physics and Astronomy School, University of Southampton, Highfield, Southampton SO171BJ, United Kingdom
[4]Spin Optics Laboratory, State University of Saint Petersburg, 1, Ulianovskaya 198504, Russia
(Received 13 July 2013; published 23 January 2014)

We address, theoretically, the puzzling similarity observed in the thermodynamic behavior of independent clouds of cold dipolar excitons in coupled semiconductor quantum wells. We argue that the condensation of self-trapped exciton gas starts at the same critical temperature in all traps due to the specific scaling rule. As a consequence of the reduced dimensionality of the system, the scaling parameters appear to be insensitive to disorder.

DOI: 10.1103/PhysRevLett.112.036401 PACS numbers: 71.35.Lk

Introduction.—The ring-shaped boundary between electron-rich and hole-rich regions in semiconductor quantum wells remote from the central hot excitation spot presents the unique setting for studying of the critical behavior in exciton gases [1]. Indirect excitons formed on the ring have extremely long lifetimes and high cooling rates which allow them to reach a thermodynamic equilibrium with the cold lattice. On the other hand, the strong repulsion of exciton dipole moments oriented perpendicularly to the plane of the structure prevents the system from the formation of biexcitons [2,3] and makes possible the observation of a Bose-Einstein condensed metastable state [4,5]. The specifics of such Bose-Einstein condensation (BEC) can be conveniently studied by analyzing the exciton photoluminescence (PL) [6,7].

Intriguing phenomena have been recently observed in the PL ring of dipolar excitons in coupled quantum wells (CQWs) [8,9] and, independently, in a biased single quantum well (SQW) structure [10]. With the lowering of temperature the exciton cloud at the ring squeezes and fragments into an array of beads seen as bright spots in the PL spectra. Shift-interferometry measurements reveal that each bead represents a macroscopically coherent exciton state (a condensate). At the same time, no phase correlations between different beads have been found [9]. These local condensates are formed in different external conditions, and their sizes vary along the ring. Indeed, though the electrostatic interaction between excitons results in screening of rapid fluctuations of the in-plane potential [11], the weak disorder varying slowly in space is always present. The effect of disorder on the formation of patterns of exciton condensates is a challenging problem which has not been addressed until now.

In this Letter we show that the pronounced dispersion of sizes of the beads observed in the experiment [8–10] can be described as accounting for a *weak* and smooth disorder potential in the system. Surprisingly, the disorder does not affect the value of the critical temperature T_c: BEC starts in all the traps simultaneously, at the same temperature as in the disorder free system. The situation resembles one in multiband superconductors: in spite of the diversity of coherence lengths and gaps of the Cooper pairs in different bands at relatively low temperatures, the system unifies close to the phase transition, and the transition occurs at a unique critical temperature. This important result of our model is consistent with the experimental studies [8–10].

In the absence of interactions and disorder, the cloud of indirect excitons localized at the ring would condense homogeneously at some temperature corresponding to zero chemical potential. However, the time to reach kinetic equilibrium and build up the long-range order in such an ideal gas would be infinitely long [12]. The strong dipole-dipole repulsion between excitons ensures fast thermalization of the whole cloud, but BEC occurs at a lower critical temperature T_c and would result in fragmentation of the ring into a perfectly periodic array of localized condensates [13]. In the thermodynamic limit, the number of beads would be determined by the balance between the kinetic and entropy terms in the free energy of the exciton system [14]. The exciton bead density profile along the ring reproduces the shape of the *self-trapping* potential. The latter can be assumed to be of a harmonic type for all beads:

$$V_j(x,y) = \frac{1}{2}m\omega_j^2 x^2 + \frac{1}{2}m\omega_y^2 y^2, \tag{1}$$

where x corresponds to the azimuthal and y to the radial direction, $j = 1, 2, \ldots, J$ is the index of the bead and, in the absence of disorder, $\omega_1 = \omega_2 = \ldots \equiv \omega_x$ [15]. Localization of the clouds in the radial direction y is due to the macroscopic in-plane charge separation (see Fig. 1 and Ref. [16]). The chemical potential of each independent

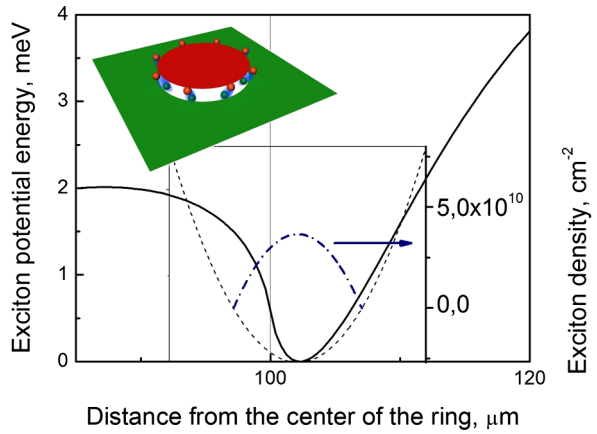

FIG. 1 (color online). Calculated potential profile for the radial motion of an indirect exciton in the vicinity of the ring (solid line) and the model harmonic trap (dashed line). Details of the calculation can be found in [16]. The localization is due to the macroscopic charge separation (color inset on the left) which induces an in-plane electric field. The field tilts the exciton dipoles and thus reduces their potential energy. At low temperatures, excitons condense at the potential minimum located near the charge boundary. As a consequence of strong repulsive interactions, the density profile of the exciton condensate is very smooth and merely reproduces the shape of the trap (dotted-dashed line).

cloud μ_j can be calculated using the normalization condition

$$N_j(\mu_j) = \int n_j(x, y, \mu_j) dxdy, \tag{2}$$

where $n_j(x, y, \mu_j)$ is the density profile of this cloud [see Eq. (7) below],

$$\sum_j N_j(\mu_j) = N_0, \tag{3}$$

with N_0 being the total number of excitons at the ring in a steady state, and

$$\mu_1 = \mu_2 = \cdots \equiv \mu, \tag{4}$$

so that the three equations (2), (3), and (4) determine, in fact, the unique chemical potential μ of the interacting disorder free system.

The effect of disorder can be studied considering a perturbative correction to the self-induced part of the localizing potential: the potential traps (1) acquire different curvature (characterized by ω_j) and contain a different number of excitons N_j, while the chemical potential μ defined by (2) remains unchanged and the condition of kinetic equilibrium (4) is not violated [17]. Below we show, that at the experimentally achieved exciton densities, the latter implies that the critical point T_c is not affected by disorder and remains unique for the whole system. To obtain this nontrivial result we extend the principle of *scale invariance* on a two-dimensional harmonically trapped gas and show that all the beads belong to the same *universality class*.

Scale invariance.—Self-trapping along the ring alters dramatically the density of exciton states, making it possible to observe the true second order phase transition in the thermodynamic limit. In this case the scale invariance, generally taking place in the critical region [18], was shown to be extended down to zero temperature [19,20]. A physical reason for this specific scaling is quenching of finite size effects (negligibility of the kinetic energy term in the mean field equation for a condensate) [19]. The relevant thermodynamic functions of a trapped cloud can be expressed in terms of two parameters: the critical temperature of BEC of noninteracting particles in a harmonic trap $T^0_{c,j}$ and the ratio $\eta_j = \mu_j(T = 0)/k_B T^0_{c,j}$. In what follows we show that the scaling parameters are the same for all localized exciton clouds.

By analogy with a three-dimensional problem [19,20], the thermodynamic limit for a two-dimensional harmonically trapped gas can be formally obtained by letting the total number of particles N_j in a trap increase to infinity, and the oscillator frequency $\omega_{ho,j} = (\omega_j \omega_y)^{1/2}$ decrease to zero, while keeping fixed the product $\omega_{ho,j} N_j^{1/2}$. The latter defines the critical temperature of an ideal gas in a harmonic trap

$$k_B T^0_{c,j} = (6/\pi^2)^{1/2} \hbar \omega_{ho,j} N_j^{1/2}. \tag{5}$$

To account for contact interactions between the excitons in the trap domain, we take advantage of the fact [12] that as $\omega_{ho,j} \to 0$ the density profile of the jth cloud $n_j(x, y)$ is fixed by the condition of local equilibrium

$$\bar{\mu}[n_j(x, y), T] = \mu_j(T) - V_j(x, y). \tag{6}$$

Here $\bar{\mu}(\bar{n}, T)$ is the value of a *local* chemical potential calculated for a *uniform* system having the density $\bar{n} = n_j(x, y)$, while $\mu_j(T)$ is the chemical potential of the cloud. By inverting the condition (6) one can write the density $n_j(x, y)$ in the form

$$n_j(x, y) = \bar{n}[\mu_j(T) - V_j(x, y), T], \tag{7}$$

where $\bar{n}(\bar{\mu}, T)$ is merely the density of the uniform gas expressed in terms of its chemical potential and temperature. At $T = 0$ one would obtain the well-known Thomas-Fermi result for the condensate:

$$n_j(x, y, T = 0) = \frac{1}{V_0}[\mu_j(T = 0) - V_j(x, y)]\theta[\mu_j(T = 0) - V_j(x, y)], \tag{8}$$

where $\theta(x)$ is the Heaviside step function. In practice, tracing the local value of the chemical potential $\bar{\mu}(x, y)$

allows one to reproduce the density profile of a cloud and vice versa [21].

Using the normalization condition (2) and Eq. (8) one finds the chemical potential at $T = 0$ in the form

$$\mu_j(T=0) = \sqrt{\frac{mV_0}{\pi\hbar^2}}\hbar\omega_{ho,j}N_j^{1/2}, \tag{9}$$

and the ratio

$$\eta_j \equiv \frac{\mu_j(T=0)}{k_B T_{c,j}^0} = \sqrt{\frac{\pi}{6}\frac{mV_0}{\hbar^2}}. \tag{10}$$

Crucially, in contrast to the case of a three-dimensional gas [19], the quantities η_j in (10) are not dependent on the oscillator frequencies ω_j and ω_y characterizing the trap and on the number of particles in a cloud N_j. Providing that the condition (4) is satisfied, this implies that the critical temperature of an ideal gas $T_{c,j}^0$ is also the same for all traps, so that one can write

$$\eta_1 = \eta_2 = \cdots \equiv \eta, \tag{11a}$$

$$T_{c,1}^0 = T_{c,2}^0 = \cdots \equiv T_c^0. \tag{11b}$$

In order to show that the quantities η and T_c^0 are the scaling parameters, we follow Ref. [12] and introducing a new variable $\xi \equiv V_j(x,y)$ rewrite the identity (2) in the form [16]

$$2(k_B T_c^0)^{-2}\int \frac{6}{\pi}\frac{\hbar^2}{m}\bar{n}(\mu-\xi,T)d\xi = 1, \tag{12}$$

where we have used Eq. (7) with μ_j replaced by μ according to (4). Inversion of the equation (12) yields the general dependence $\mu = \mu(T, T_c^0, \eta)$ for the chemical potential of the trapped cloud. Because of the dimensionality arguments this expression can be recast in the form

$$\mu = k_B T_c^0 f(t,\eta), \tag{13}$$

where $t \equiv T/T_c^0$ is the reduced temperature, f is a generic function which satisfies $f(0,\eta) = \eta$.

Equation (13) exhibits the anticipated scaling in terms of η and T_c^0. By analogy, one can show the scaling of all other thermodynamic functions. Having in mind the result (11) one can conclude that all the beads belong to the same universality class defined by η and T_c^0. In particular, the critical point is unique for the whole system even in the presence of disorder. To illustrate this important result, let us estimate $T_c(\eta, T_c^0)$ for a small η, where the simplest Hartree-Fock scheme can be applied [20]. In this approximation,

$$f(t,\eta) = \eta(1-t^2)^{1/2} \tag{14}$$

and T_c can be found solving the transcendental equation $\mu(T_c, T_c^0, \eta) = \epsilon[\mu(T_c, T_c^0, \eta), T_c]$ with ϵ being the lowest eigenvalue of the single particle Hamiltonian $H_{\mathrm{sp},j} = V_j(x,y) + 2V_0 n_j(x,y)$. Using Eqs. (7), (13), and (14) one finds [16]

$$T_c = T_c^0\left(1 + \frac{x^2(\eta)}{\eta^2}\right)^{-1/2}, \tag{15}$$

where $x(\eta)$ is a root of $\pi^2 x = 6\eta^2\mathrm{Li}(e^{-x})$, $\mathrm{Li}(x)$ is the Eulerian logarithmic integral [22].

The scaling arguments given above are based on the local density approximation (LDA) given by Eq. (7) or, equivalently, (6). Experimental [21] and *ab initio* [23] studies show that LDA for 2D gases is already valid to a good accuracy for $\sim 10^4$ particles. This corresponds to the experimentally achieved exciton densities in a bead [8]. However, since an exciton gas is quite different from usual atomic gases, it is worth discussing the applicability of LDA for the beads in details.

The validity of the local density approximation for the beads.—To verify the validity of the Thomas-Fermi approximation for exciton clouds, we notice that the local chemical potential $\bar{\mu}(x,y)$ given by Eq. (6) can be inferred from the PL energy profiles along the ring measured in [7] and shown there in Fig. 2. Indeed, the chemical potential $\bar{\mu}(x,y)$ contributes to the energy of a photon emitted by an exciton during recombination. Neglecting the thermal component of the exciton gas, the average PL energy measured in [7] for one bead can be written as

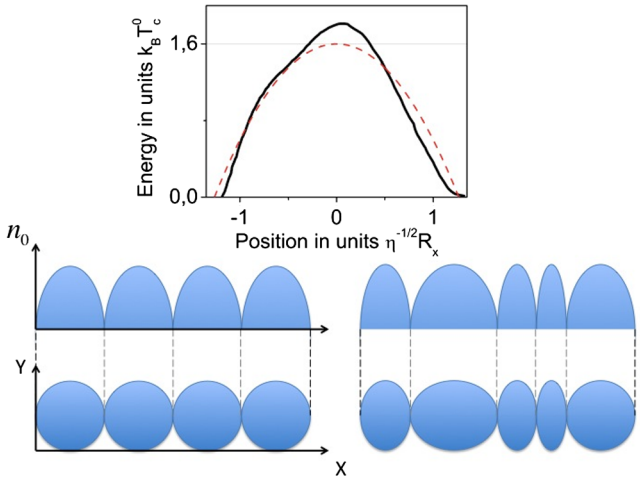

FIG. 2 (color online). (top) The $T = 0$ Thomas-Fermi result $\bar{\mu}/k_B T_c^0 = \eta - \tilde{x}^2$ for the variation of exciton energy along the ring ($\tilde{x}$ axis) at $\tilde{y} = 0$ (the dashed red line). The exciton resonance position measured in [7] from PL spectra is shown by the solid line. The scaling parameters are $\eta = 1.6$ and $T_c^0 = 4.5$ K. The Thomas-Fermi radius of the bead is measured to be $R_x = 20$ μm. (Bottom) The topological transformation of the condensate density given by (19) conserving the total number of particles $N_0 = \int n_0 dxdy$ and the Thomas-Fermi energy $E_{\mathrm{TF}} = V_0\int n_0^2 dxdy$.

$$E_{\mathrm{PL}}(x) - \mathrm{const} = \frac{\int \bar{\mu}(x,y)n(x,y)dy}{\int n(x,y)dy} = \frac{4}{5}\bar{\mu}(x,y=0), \tag{16}$$

with $n(x,y)$ given by (8) where we have omitted the index j for simplicity (this change in the notation will be kept until the end of this section). We choose a bead in the middle of Fig. 2 of Ref. [7], which has the most regular shape compared to its neighbours. When expressed in reduced units and multiplied by $5/4$ to account for the averaging along y axis [Eq. (16)], the energy profile of this bead reads $\bar{\mu}/k_B T_c^0 = \eta - \tilde{x}^2$ [Fig. 2], where $\tilde{x} = \eta^{1/2}x/R_x$ and

$$R_x = [2\mu(T=0)/m\omega_x^2]^{1/2} \tag{17}$$

is the Thomas-Fermi radius. Here we have substituted $\mu(T=0) = \eta k_B T_c^0$ into the right-hand side of Eq. (6). Note, that we do not adjust the scaling parameters: we find $\eta = 1.6$ using Eq. (10), where we substitute $V_0 = 1.7\ \mu\mathrm{eV} \times \mu\mathrm{m}^2$ calculated using the plate capacitor formula with the correction factor [3]. In what concerns the parameter T_c^0, it can be estimated from the experimental temperature at which the fragmentation and the build up of the extended coherence occur $T_c^0 = 4.5$ K [7].

Furthermore, using the Thomas-Fermi approximation (17) for available values of the parameters η and T_c^0 one can estimate the oscillator frequency ω_y of the radial localizing potential which would correspond to the experimentally observed ring width $2R_y \sim 10\ \mu$m. Remarkably, this potential can be obtained from the first principles, see [16]. The result of this calculation is shown in Fig. 1 by a solid line. The input parameters for the calculation procedure correspond to those typical of the experiment. The dashed line shows the model harmonic potential. We also plot the ground state density profile for $\eta = 1.6$ and $T_c^0 = 4.5$ K (we have assumed $\omega_x = \omega_y$ for simplicity). As one could expect, the semiclassical condition $\hbar\omega_y \ll k_B T_c^0$ is well satisfied.

The energy scale of the disorder.—Finally, let us estimate the energy scale of the disorder potential which can induce the significant dispersion of bead sizes observed in practice. We do not wish to complicate the issue by taking into account the thermal component of the gas and, therefore, consider the fragmented exciton condensate at $T = 0$. As we have already explained, in the scaling regime this restriction does not imply any loss of generality.

It is reasonable to assume that at $T = 0$ the adjacent condensates touch each other as it is shown schematically in Fig. 2 (in order to minimize the interaction energy E_{TF}). In the Thomas-Fermi limit this means that the oscillator frequencies $\{\omega_j\}$ satisfy the " continuity" condition

$$\sum_j [2\mu(T=0)/m\omega_j^2]^{1/2} = \pi R, \tag{18}$$

where R is the ring radius. The smooth disorder can fragment the condensate and vary the size of the beads along the ring, while conserving the parabolic shape of the bead density profiles $n_j(x,y,T=0)$. Interestingly, such topological transformation of the exciton density can be formally achieved by the replacement

$$\{\omega_j\} \to \{\omega_k\}^*, \tag{19}$$

where $\{\omega_k\}^*$ is a new set of oscillator frequencies, $k = 1, 2, \ldots, K$, satisfying the condition (18) with k instead of j and $K \neq J$ in general. One can check [16] that the transformation (19) conserves the total number of particles N_0 [Eq. (3)].

This way, one can achieve the pronounced dispersion of the bead sizes observed experimentally maintaining the chemical potential $\mu(T=0)$ corresponding to *the disorder free system*. This suggests that the variation of the disorder potential δ on the scale of the bead size is much less than $\mu(T=0)$. Indeed, not only the sum $\sum_j \int n_j(x,y,T=0)dxdy = \mathrm{inv}$ but also

$$\sum_j \int n_j^2(x,y,T=0)dxdy = \mathrm{inv} \tag{20}$$

under the topological transformation defined by (19). Equation (20) defines the energy accumulated in the clouds due to the repulsive interaction (the Thomas-Fermi energy) $E_{\mathrm{TF}} = V_0 \sum_j \int n_j^2(x,y,T=0)dxdy$. To estimate the lowest bound for δ one should go beyond the scaling limit. It is shown in Ref. [14] that the kinetic energy correction to the Thomas-Fermi approximation can be estimated as $k_B T_c^0/\eta$ (per one bead). Therefore, it is sufficient to introduce a weak disorder which varies smoothly by

$$k_B T_c^0/\bar{N}_j\eta < \delta \ll \mu(T=0) \equiv \eta k_B T_c^0 \tag{21}$$

on the scale of the bead size so that one could observe its effect on the fragmented exciton condensate ($\bar{N}_j$ is the average number of particles in a bead). The high sensitivity of condensate sizes to the disorder reflects the fact that the trapping potential along the ring is essentially self-induced.

Conclusions.—We have shown that the fragmented exciton ring represents an array of trapped Bose-Einstein condensates close to the thermodynamical limit. The relevant thermodynamic functions of exciton clouds exhibit scaling in terms of the parameters η and T_c^0. With lowering the temperature, the lakes of condensed excitons grow maintaining the same chemical potential. The dispersion of their sizes reveals weak and smooth structural disorder, which is hidden from an observer above T_c. As a consequence of the reduced dimensionality, such disorder does not alter the scaling parameters. This explains the experimentally observed universality in the thermodynamic behavior of statistically independent exciton condensates.

S. V. is grateful to K. V. Kavokin for fruitful discussion on the existence of the in-plane radial trap for excitons. A. V. acknowledges the support of the EU IRSES project SIMTECH No. 246937, A. K. acknowledges support from the Russian Ministry of Education and Science, Grant No. N11.G34.31.0067.

*Sergey.Andreev@univ-montp2.fr

[1] L. V. Butov, L. S. Levitov, A. V. Mintsev, B. D. Simons, A. C. Gossard, and D. S. Chemla, Phys. Rev. Lett. **92**, 117404 (2004).
[2] A. V. Gorbunov and V. B. Timofeev, JETP Lett. **96**, 138 (2012).
[3] C. Schindler and R. Zimmermann, Phys. Rev. B **78**, 045313 (2008).
[4] L. V. Keldysh and A. N. Kozlov, Sov. Phys. JETP **27**, 521 (1968).
[5] The phase diagram showing the critical temperature of condensation of indirect excitons in a trap as a function of their density is reported in [2]. The spatial separation of electrons and holes is crucial for debarment of formation of the excitonic molecules (biexcitons) which prevents the Bose-Einstein condensation of excitons in single unbiased quantum wells. Biexcitons cannot be formed if the dipole-dipole repulsion of excitons is strong enough, which implies the electron-hole separation by several nanometers. On the other hand, the excitons themselves remain stable at this condition. The exciton binding energy does not drop down significantly until the distance between quantum wells exceeds the exciton Bohr diameter, which is of the order of 20 nm in GaAs based quantum wells.
[6] L. V. Butov, J. Phys. Condens. Matter **19**, 295202 (2007).
[7] S. Yang, A. V. Mintsev, A. T. Hammack, L. V. Butov, and A. C. Gossard, Phys. Rev. B **75**, 033311 (2007).
[8] L. V. Butov, A. C. Gossard, and D. S. Chemla, Nature (London) **418**, 751 (2002).
[9] A. A. High, J. R. Leonard, A. T. Hammack, M. M. Fogler, L. V. Butov, A. V. Kavokin, K. L. Campman, and A. C. Gossard, Nature (London) **483**, 584 (2012).
[10] M. Alloing, D. Fuster, Y. Gonzalez, L. Gonzalez, and F. Dubin, arXiv:1210.3176.
[11] A. L. Ivanov, Europhys. Lett. **59**, 586 (2002).
[12] L. Pitaevskii and S. Stringari, *Bose-Einstein Condensation* (Clarendon Press, Oxford, 2003).
[13] Noteworthy, before the recent experimental studies that have shown that the macroscopically ordered exciton state is characterized by strong repulsive interaction [7] and evidenced its coherent nature [9], there were attempts to explain the fragmentation in terms of classical models assuming the two-body attraction between excitons [see C. S. Liu, H. G. Luo, and W. C. Wu, J. Phys. Condens. Matter **18**, 9659 (2006) and references therein].
[14] S. V. Andreev, Phys. Rev. Lett. **110**, 146401 (2013).
[15] Strictly speaking, the self-trapping potential oscillates along the ring and can be characterized by $\{\omega_j\}$ only in the vicinity of its local minima. The local harmonic potential approximation (1) is valid if the traps are deep enough and a large part of noncondensed excitons is effectively localized in each site j. This is the case in the experiments [8,9].
[16] See Supplemental Material at http://link.aps.org/supplemental/10.1103/PhysRevLett.112.036401 for full details of all derivations.
[17] Below T_c the kinetic equilibrium is reached on a time scale of inverse temperature due to strong fluctuations of the relative phases between the adjacent condensates. The fluctuations result in damping of coherent exciton flows, which would be induced if the condition (4) is violated. Such a damping mechanism is well known in the physics of superconductors, where the fluctuations of the phase in Josephson junctions result in energy dissipation and decay of supercurrents. At higher temperatures the fluctuations are due to thermal activation of the phase, while close to absolute zero they are of quantum nature and, in terms of mechanical analogy, correspond to the tunneling of the phase between the neighboring condensates [24].
[18] L. Kadanoff, W. Götze, D. Hamblen, R. Hecht, E. Lewis, V. Palciauskas, M. Rayl, J. Swift, D. Aspnes, and J. Kane, Rev. Mod. Phys. **39**, 395 (1967).
[19] S. Giorgini, L. P. Pitaevskii, and S. Stringari, Phys. Rev. Lett. **78**, 3987 (1997).
[20] S. Giorgini, L. P. Pitaevskii, and S. Stringari, J. Low Temp. Phys. **109**, 309 (1997).
[21] C.-L. Hung, X. Zhang, N. Gemelke, and C. Chin, Nature (London) **470**, 236 (2011).
[22] M. Abramowitz and I. A. Stegun, *Handbook of Mathematical Functions with Formulas, Graphs, and Mathematical Tables* (Dover, New York, 1965).
[23] S. P. Cockburn and N. P. Proukakis, Phys. Rev. A **86**, 033610 (2012).
[24] A. Larkin and A. Varlamov, *Theory of Fluctuations in Superconductors* (Oxford University Press, New York, 2005).